Letter

Alleviating the Hubble-constant tension and the growth tension via a transition of absolute magnitude favored by the Pantheon+ sample

Yang Liu,[1,‡] Hongwei Yu,[1,2,*] and Puxun Wu[1,2,†]

[1]*Department of Physics and Synergetic Innovation Center for Quantum Effects and Applications, Hunan Normal University, Changsha, Hunan 410081, China*

[2]*Institute of Interdisciplinary Studies, Hunan Normal University, Changsha, Hunan 410081, China*

(Received 29 January 2024; accepted 4 June 2024; published 22 July 2024)

We establish a cosmological-model-independent method to extract the apparent magnitude and its derivative at different redshifts from the Pantheon+ type Ia supernova sample and find that the obtained values deviate clearly from the prediction of the ΛCDM model at the lowest redshift. This deviation can be explained as a result of a transition of the absolute magnitude M in the low-redshift region. The observations seem to favor this transition, since the minimum values of χ^2 for two *Ansätze* of a varying M are less than that of a constant M. The Hubble-constant tension is alleviated from larger than 5σ to be about 1σ–2σ for a varying M, and the growth tension can be resolved after attributing the variation of M to a modification of the effective Newton's constant.

DOI: 10.1103/PhysRevD.110.L021304

Introduction. The cosmological constant Λ plus cold dark matter (ΛCDM) is the simplest and most popular cosmological model. It is well consistent with many observations, on one hand, but, on the other hand, it still suffers the serious Hubble-constant (H_0) tension [1–3], which refers to a more than 5σ disagreement between the measurements of H_0 given, respectively, by the SH0ES Collaboration [4] and the *Planck* satellite [5]. Within the framework of the ΛCDM model, the cosmic microwave background (CMB) radiation data from the *Planck* satellite infer $H_0 = 67.4 \pm 0.5\ \mathrm{km\,s^{-1}\,Mpc^{-1}}$ [5], which deviates significantly from $H_0 = 73.04 \pm 1.04\ \mathrm{km\,s^{-1}\,Mpc^{-1}}$ constrained cosmological-model-independently by the data from the nearby type Ia supernovae (SNe Ia) [4]. These SNe Ia are calibrated by using the Cepheids according to the idea of a distance ladder, and the absolute magnitude M of SNe Ia is determined to be $M = -19.253 \pm 0.027$ mag. To figure out whether the H_0 tension originates from the calibration of SNe Ia, the Mira variables have been used to calibrate the SNe Ia, resulting in $M = -19.27 \pm 0.13$ mag, which yields $H_0 = 72.7 \pm 4.6\ \mathrm{km\,s^{-1}\,Mpc^{-1}}$ [6]. This result is consistent with that from the Cepheid-calibrated SNe Ia, while it is larger than $H_0 = 69.8 \pm 1.7$ and $70.50 \pm 4.13\ \mathrm{km\,s^{-1}\,Mpc^{-1}}$ obtained, respectively, from the SNe Ia calibrated with the tip of the red giant branch [7] and the surface brightness fluctuations [8]. However, if the idea of an inverse distance ladder and the high-redshift data, such as the baryon acoustic oscillation, are utilized to calibrate the SNe Ia, a value of M smaller than that from the Cepheids and a value of H_0 consistent with that from the Planck CMB data are achieved [9,10]. Apparently, a smaller M seems to give a smaller H_0. Thus, the H_0 tension can also be regarded as the M tension [11].

The H_0 tension may be caused by either systematic errors or local bias. Unfortunately, no systematics, which could explain this tension, have been found so far [12–22], and a local void cannot save the tension either [23–26]. Therefore, the H_0 tension may be the smoking gun of new physics beyond the ΛCDM model in either the early or late Universe [27]. A simple extension of the ΛCDM model in the late Universe is to replace the cosmological constant with a dynamical dark energy, such as that described by the Chevalier–Polarski–Linder (CPL) parameterization. However, these extensions cannot fully solve the tension [28–31], since they only enlarge the uncertainties of the constraints on the cosmological parameters. Noteworthily, reducing the cosmic sound horizon, which can be realized by modifying the recombination history or introducing an early dark energy [32–35], seems to be capable of resolving the H_0 tension, but it may regrettably worsen the so-called growth tension at the same time [36,37]. This tension refers to the about 3σ disagreement between the values of the matter density parameter Ω_{m0} and the parameter σ_8 constrained, respectively, from the Planck 2018 CMB data [5] in the ΛCDM background geometry and the dynamical probes of the cosmological perturbations including cluster counts [38–41], weak lensing [42–49], and redshift-space distortions [50–54]. Here, σ_8 is defined as the matter density rms fluctuations in spheres of radius $8h^{-1}$ Mpc at $z = 0$ with

*Contact author: hwyu@hunnu.edu.cn
†Contact author: pxwu@hunnu.edu.cn
‡Contact author: yangl@hunnu.edu.cn

 © 2024 American Physical Society

$h \equiv \frac{H_0}{100\ \mathrm{km\,s^{-1}\,Mpc^{-1}}}$. Therefore, the Hubble-constant tension remains an open issue in modern cosmology.

A possible way to find out the origin of the H_0 tension is to probe directly the cosmic background dynamics from the observational data. In this paper, we propose a model-independent method to extract the apparent magnitude m and its derivative $m' = \frac{dm}{dz}$ at different redshift points from the latest Pantheon+ SNe Ia sample [55]. We find that, except for the results at the lowest redshift point, the obtained values of m and m' are very well compatible with the prediction from the ΛCDM model. Thus, it is reasonable to assume that the ΛCDM model can describe correctly the cosmic evolution, and the deviation of m and m' from the prediction of the ΛCDM model at the low-redshift region originates from a transition of the absolute magnitude M of SNe Ia. We demonstrate that such a transition of M will alleviate the H_0 tension. If the transition of M is further assumed to arise from the variation of the effective Newton's constant G_{eff}, the growth tension can be resolved, too.

Values of apparent magnitude and its derivative. One observable of SNe Ia is the apparent magnitude $m(z)$. Its theoretical value relates to the cosmological model through

$$m_{\mathrm{th}}(z) = 25 + 5\log_{10}\left(\frac{D_L(z)}{\mathrm{Mpc}}\right) + 5\log_{10}\left(\frac{c}{H_0}\right) + M. \quad (1)$$

Here, c is the speed of light, and $D_L(z)$ is the dimensionless luminosity distance, which is defined as $D_L(z) \equiv (1+z)\int_0^z \frac{dz'}{E(z')}$ in a spatially flat universe, where $E(z)$ is the dimensionless Hubble parameter and $E(z) \equiv \sqrt{\Omega_{\mathrm{m0}}(1+z)^3 + (1-\Omega_{\mathrm{m0}})}$ for the ΛCDM model. Comparing the observed $m(z)$ with its corresponding theoretical value can give constraints on the cosmological models with the SNe Ia data, e.g., $\Omega_{\mathrm{m0}} = 0.333 \pm 0.018$ in the ΛCDM model with the Pantheon+ SNe Ia sample, which comprises 1701 light curves with 1550 distinct SNe Ia and spans to redshift $z \simeq 2.26$ [55]. If a prior on M is further given, a constraint on H_0 will be achieved by using SNe Ia. With $M = -19.253 \pm 0.027$ mag from the Cepheids, the Pantheon+ SNe Ia sample gives $H_0 = 73.22 \pm 0.95\ \mathrm{km\,s^{-1}\,Mpc^{-1}}$ in the ΛCDM model.

To model-independently probe the local background dynamics of our Universe with the Pantheon+ sample, we now establish a local expansion method, which is to expand the apparent magnitude $m(z)$ at a given redshift. We do the Taylor expansion of $m(z)$ in the $\ln z$ space instead of the z space, to the first order:

$$m(z) = m_i + z_i m_i'(\ln z - \ln z_i), \quad \text{if } z_{\mathrm{min},i} < z \le z_{\mathrm{max},i}, \quad (2)$$

where $m_i \equiv m(z_i)$, $m_i' \equiv \frac{dm}{dz}|_{z=z_i}$, and z_i is the redshift point where the expansion is performed, which is determined by using $\ln z_i = (\ln z_{\mathrm{min},i} + \ln z_{\mathrm{max},i})/2$ in our analysis.

We consider the Pantheon+ SNe Ia sample and use the Hubble diagram redshift z_{HD}, which is derived from the CMB frame redshift (z_{CMB}) with corrections from the peculiar velocity, as the redshift z of the Pantheon+ sample. We exclude those data points whose redshifts are less than 0.01, since the nearby sample may be impacted by their peculiar velocities [56]. Furthermore, we also ignore the data with the redshift $z > 0.8$, since only 30 data points lie in the redshift region $z \in (0.8, 2.26]$. Thus, the remaining 1560 data points are used in our analysis. We divide these data into five bins with the same number of data points in each bin. As there are two free parameters (m_i and m_i') in each bin, we have totally ten free parameters. These parameters are constrained by minimizing the following χ^2:

$$\chi^2 = \left[\hat{\boldsymbol{m}}_{\mathrm{obs}} - m(z)\right]^{\dagger} C_{\mathrm{SN}}^{-1} \left[\hat{\boldsymbol{m}}_{\mathrm{obs}} - m(z)\right] \quad (3)$$

from the Pantheon+ SNe Ia data. Here, C_{SN} is the covariance matrix of 1560×1560, which is a submatrix of the full SNe Ia sample, and $\hat{\boldsymbol{m}}_{\mathrm{obs}}$ is the 1D array consisting of the SNe Ia apparent magnitudes. Ten free parameters, i.e., m_i and m_i' with i varying from 1 to 5, are simultaneously fitted by using the Markov chain Monte Carlo (MCMC) method. Before using the real data to constrain these free parameters, we need to check the reliability of our method. To do so, we first mock 1560 SNe Ia data points in the redshift region of $0.01 \le z \le 0.8$ with the value of $\langle m_{\mathrm{th}} \rangle$ from the fiducial model: the ΛCDM model ($\Omega_{\mathrm{m0}} = 0.333$, $H_0 = 73.22\ \mathrm{km\,s^{-1}\,Mpc^{-1}}$, and $M = -19.253$ mag), and the same redshift distribution as that of the Pantheon+ sample. The mock data are divided into four, five, and six bins with the same number of points in each bin, respectively. Then, the best-fitting values of m_i and m_i' in each bin from the mock data can be estimated by using the minimum χ^2 method. We repeat our analysis 1000 times and find that the mean values of m_i and m_i' are well consistent with those derived from the fiducial model for the cases of five and six bins. Thus, the simulation analysis shows that the results from real data will be reliable if the bin number is larger than four. The detailed discussions can be found in the Supplemental Material Ref. [57].

Table I lists the constraints on m_i and m_i' in each bin and on $\Delta m_i \equiv m_i - m_{i,\mathrm{th}}$ and $\Delta m_i' \equiv m_i' - m_{i,\mathrm{th}}'$, which represent the differences between the values from the Pantheon+ sample and the prediction of the fiducial model. It is easy to see that, in the last four bins, the constraints on m_i and m_i' are very well consistent with those of the fiducial model. However, in the first bin ($z_1 = 0.017$), the value of Δm_1 is compatible with zero at 2σ confidence level (CL), whereas $\Delta m_1'$ deviates from zero at about 2.7σ.

TABLE I. Expanding redshift point z_i, number of SNe Ia, and constraints on m_i and m_i'. The mean values with 1σ uncertainty are shown. Δm_i ($\Delta m_i'$) denote the differences between the constraints on m_i (m_i') and the fiducial model: ΛCDM model with $\Omega_{m0} = 0.333 \pm 0.018$ and $\mathcal{M} = 25 + 5\log_{10}(\frac{c}{H_0}) + M = 23.808 \pm 0.007$.

Pantheon+ sample with z_{HD}					
	Bin 1	Bin 2	Bin 3	Bin 4	Bin 5
z_i	0.017	0.049	0.144	0.296	0.544
Redshift range	$0.010 < z \leq 0.027$	$0.027 < z \leq 0.087$	$0.087 < z \leq 0.237$	$0.237 < z \leq 0.370$	$0.370 < z \leq 0.799$
N_{SN}	312	312	312	312	312
m_i	14.955 ± 0.015	17.338 ± 0.009	19.800 ± 0.010	21.563 ± 0.008	23.088 ± 0.011
m_i'	125.735 ± 2.571	45.468 ± 0.511	16.530 ± 0.223	8.543 ± 0.202	4.704 ± 0.076
Δm_i	0.024 ± 0.016	0.006 ± 0.011	-0.003 ± 0.013	0.006 ± 0.014	-0.017 ± 0.020
$\Delta m_i'$	-6.894 ± 2.571	-0.463 ± 0.512	0.084 ± 0.224	0.146 ± 0.203	-0.072 ± 0.079
Pantheon+ sample with z_{CMB}					
z_i	0.016	0.049	0.146	0.296	0.544
Redshift range	$0.010 < z \leq 0.027$	$0.027 < z \leq 0.090$	$0.090 < z \leq 0.237$	$0.237 < z \leq 0.371$	$0.371 < z \leq 0.799$
N_{SN}	312	312	312	311	311
m_i	14.957 ± 0.015	17.378 ± 0.009	19.846 ± 0.010	21.564 ± 0.008	23.093 ± 0.011
m_i'	126.639 ± 2.606	44.275 ± 0.497	16.228 ± 0.212	8.484 ± 0.197	4.686 ± 0.075
Δm_i	0.037 ± 0.016	0.019 ± 0.012	0.000 ± 0.013	0.006 ± 0.014	-0.013 ± 0.019
$\Delta m_i'$	-6.689 ± 2.606	-1.114 ± 0.498	0.048 ± 0.214	0.083 ± 0.198	-0.091 ± 0.078

For a more comprehensive comparison between the observed and simulated datasets, we extended our analysis to include cases with four and six bins. The results obtained from the Pantheon+ SNe Ia data are presented in Tables I and II in the Supplemental Material Ref. [57], respectively. In both cases, the values of $\Delta m_1'$ from the observed data are inconsistent with zero at more than 2σ CL. This result is different from what is obtained from the mock data, but it is similar to the five-bin result. And all other results are compatible with the prediction of the fiducial model at 2σ CL.

We also study the possible volume effect in the redshift region $0.01 < z \leq 0.027$ and find that it cannot fully account for the deviation of Δm_1 and $\Delta m_1'$. The volume effect here refers to the bias on the low-redshift Hubble diagram of SNe Ia caused by the peculiar velocities of high-redshift SNe Ia host galaxies. This bias arises because the number density of galaxies per unit distance generally increases as the square of distance. Consequently, the number density of SNe Ia per unit distance at higher redshifts is larger than that at lower redshifts. Therefore, more SNe Ia located at higher redshifts and within a greater volume will be scattered down to lower redshifts under the influence of their host galaxies' peculiar velocities, compared to the reverse scenario [56,58,59]. To clearly demonstrate the impact of peculiar velocities on our analysis, we consider the Pantheon+ type Ia supernovae (SNe Ia) sample, using the CMB frame redshift (z_{CMB}) instead of the Hubble diagram redshift (z_{HD}). This sample comprises 1558 data points within the redshift range of $0.01 < z < 0.8$. The findings are detailed in the lower part in Table I. When comparing results derived using z_{CMB} with those using z_{HD}, we observe that the constraints on parameters m_i and m_i' for $i \geq 3$ remain largely unaffected by the choice of redshift, consistently aligning with the predictions of the fiducial model. However, the parameters Δm_2 and $\Delta m_2'$, which align with zero within 1σ CL when using z_{HD}, deviate from zero beyond 1σ CL with z_{CMB}, with the deviation of $\Delta m_2'$ reaching 2.24σ. Additionally, while the deviation of Δm_1 from zero becomes more significant, increasing from just over 1σ to more than 2σ, the value of $\Delta m_1'$ remains similar to that obtained using z_{HD}. This analysis highlights that the deviations of Δm_1 and $\Delta m_1'$ from zero are robust to the choice of redshift. Therefore, our results show that in the low-redshift region the Pantheon+ SNe Ia data support the deviation of cosmic evolution from the prediction of the ΛCDM model.

A variation of absolute magnitude. We have found that the ΛCDM model is inconsistent with the SNe Ia observations only in the low-redshift region. Thus, it seems to be a reasonable assumption that the ΛCDM model provides a correct description of the cosmic evolution. Then, Eq. (1) indicates that the discrepancy between the values of the apparent magnitude from observations and the prediction of the ΛCDM model may originate from a variation of the absolute magnitude M.

We now first consider a simple *Ansatz* that M varies suddenly by an amount of constant A at redshift z_t, i.e.,

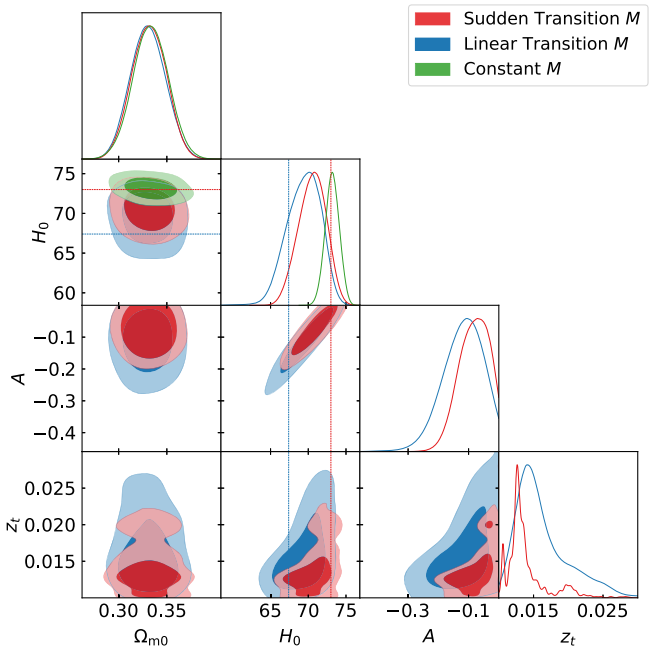

FIG. 1. Constraints on cosmological parameters and parameters describing the variation of M from the Pantheon+ SNe Ia data. The blue and red dotted lines show the constraints on H_0 from the Planck CMB and SH0ES, respectively.

$$M(z) = \begin{cases} M_0 & \text{if } z < z_t, \\ M_0 + A & \text{if } z \geq z_t, \end{cases} \tag{4}$$

where M_0 is the absolute magnitude of SNe Ia calibrated from the distance ladder, i.e., the Cepheids, and, thus, can be set to be $M_0 = -19.253 \pm 0.027$ mag. Substituting Eq. (4) into Eq. (3), we find that all m_i and m_i' will be consistent with the prediction of the ΛCDM model.

Next, we study the constraints on H_0, Ω_{m0}, A, and z_t with the Pantheon+ SNe Ia data using the MCMC method. Although parameter z_t exists only under the condition of the piecewise function and does not appear explicitly in Eq. (4), it is treated as a variable in our analysis, since the triad $\{H_0, \Omega_{m0}, A\}$ are constrained for different z_t choices. Thus, the values of H_0, Ω_{m0}, A, and z_t are sampled simultaneously. The results are shown in Fig. 1 and Table II. The best-fitting values are $\Omega_{m0} = 0.331$, $H_0 = 69.08\ \mathrm{km\,s^{-1}\,Mpc^{-1}}$, $A = -0.129$, and $z_t = 0.0126$, with $\chi^2_{\min} = 1393.3$. Their mean values with 1σ uncertainty are $\Omega_{m0} = 0.332 \pm 0.018$, $H_0 = 70.5^{+2.0}_{-1.7}\ \mathrm{km\,s^{-1}\,Mpc^{-1}}$, $A = -0.084^{+0.061}_{-0.038}$, and $z_t = 0.0139^{+0.0003}_{-0.0035}$, respectively. If $M = M_0$, we find $\Omega_{m0} = 0.333 \pm 0.018$ and $H_0 = 73.22 \pm 0.95$ with $\chi^2_{\min} = 1402.1$. Apparently, when M varies as shown in Eq. (4), the minimum of χ^2 decreases by an amount of about 8.8. The variation, however, has negligible impacts on the constraint on Ω_{m0}. The mean value of z_t shows that the transition of M occurs in the redshift region between 0.010 and 0.027, which is consistent with the result obtained in the previous section. The SNe Ia data favor a value of M smaller than M_0 at the redshift region $z \geq z_t$, since A is negative and deviates from zero at more than 1σ CL, which results in the value of H_0 smaller than $H_0 = 73.04 \pm 1.04\ \mathrm{km\,s^{-1}\,Mpc^{-1}}$ from the SH0ES Collaboration. Although the value of H_0 from the SNe Ia with a sudden variation of M still deviates slightly from that from the CMB data, this deviation reduces to be about 2σ CL. Thus, a sudden decrease of M in the low redshift region will alleviate the H_0 tension. We must point out that a transition of the SNe Ia absolute magnitude from a large value to a small one at low redshift ($z \simeq 0.01$) was first proposed in Ref. [60] to alleviate the H_0 tension. In [60], the M variation is presumed to occur at $z \simeq 0.01$ and the value ΔM, which corresponds to parameter A, is set to be -0.2 in order to fully resolve the Hubble tension. In this paper, we find a sign for this transition from the SNe Ia data, and the absolute value of A is less than 0.2.

TABLE II. Marginalized constraints on parameters in different transition models of M. The mean values with 1σ uncertainty are shown. $\Delta\mathrm{AIC(BIC)} = \mathrm{AIC(BIC)} - \mathrm{AIC_{ref}(BIC_{ref})}$, and the reference model is the constant M model.

Pantheon+ sample			
	Sudden transition	Linear transition	Constant
Ω_{m0}	0.332 ± 0.018	0.330 ± 0.018	0.333 ± 0.018
H_0	$70.5^{+2.0}_{-1.7}$	$69.4^{+2.5}_{-2.0}$	73.22 ± 0.95
A	$-0.084^{+0.061}_{-0.038}$	$-0.121^{+0.078}_{-0.052}$	⋯
z_t	$0.0139^{+0.0003}_{-0.0035}$	$0.0161^{+0.0016}_{-0.0047}$	⋯
ΔAIC(BIC)	−4.8(6)	−2.5(8.2)	0
$f\sigma_8$ sample			
Ω_{m0}	$0.286^{+0.028}_{-0.033}$	0.285 ± 0.031	$0.284^{+0.029}_{-0.032}$
σ_8	0.801 ± 0.021	$0.808^{+0.020}_{-0.023}$	0.774 ± 0.020
ΔAIC(BIC)	−0.04(−0.04)	−0.04(−0.04)	0

Since a sudden transition of M is a strong assumption, we now consider another *Ansatz* that M varies linearly with redshift in the redshift region of $z_0 \leq z < z_t$:

$$M(z) = \begin{cases} M_0 & \text{if } z < z_0, \\ M_0 + A\frac{z - z_0}{z_t - z_0} & \text{if } z_0 \leq z < z_t, \\ M_0 + A & \text{if } z \geq z_t, \end{cases} \tag{5}$$

where z_0 and z_t are two redshift points representing the beginning and ending of the variation of M, respectively. We fix $z_0 = 0.01$, since the SNe Ia data used in our analysis satisfy $z > 0.01$. Thus, we have the same free parameters (A and z_t) as in the case of a sudden variation of M. From the Pantheon+ SNe Ia data, we obtain that the best-fitting values are $\Omega_{m0} = 0.331$, $H_0 = 68.19\ \mathrm{km\,s^{-1}\,Mpc^{-1}}$,

$A = -0.156$, and $z_t = 0.0139$, with $\chi^2_{\rm min} = 1395.6$. Their mean values with 1σ uncertainty are $\Omega_{\rm m0} = 0.330 \pm 0.018$, $H_0 = 69.4^{+2.5}_{-2.0}$ km s^{-1} Mpc^{-1}, $A = -0.121^{+0.078}_{-0.052}$, and $z_t = 0.0161^{+0.0016}_{-0.0047}$, respectively. Here, the value of $\chi^2_{\rm min}$ is larger than that obtained in the case of M changing suddenly, although it is still smaller than the value in the constant M case for about 6.6. The constraint on $\Omega_{\rm m0}$ is almost the same as that in both the cases of a constant and a suddenly varying M. The mean value of z_t becomes larger slightly than the one from a sudden variation of M. The mean value of A is smaller than $A = -0.084$ obtained in the case of M varying suddenly, which leads to the value of H_0 being smaller than the one obtained by using Eq. (4) and consistent with the result from the CMB observations within 1σ. Thus, the H_0 tension is further alleviated when M varies linearly with redshift. These results can be seen clearly in Fig. 1 and Table II.

To further compare the standard model ($M = $ const) with the models with a varying M, we consider the Akaike information criterion (AIC) [61,62] and the Bayesian information criterion (BIC) [63], which are defined as $\mathrm{AIC} = 2p - 2\ln\mathcal{L}$ and $\mathrm{BIC} = p\ln N - 2\ln\mathcal{L}$, respectively. Here, p is the number of free parameters, N is the number of data points, and $\mathcal{L} \propto \exp(-\chi^2/2)$ is the likelihood function. The difference in the AIC(BIC) of a given model relative to the reference model can be calculated by using $\Delta\mathrm{AIC(BIC)} = \mathrm{AIC(BIC)} - \mathrm{AIC_{ref}(BIC_{ref})}$. Here, the model with a constant M will be set as the reference model. If $0 < |\Delta\mathrm{AIC}| < 2$, it is difficult to single out a better model, while $4 < |\Delta\mathrm{AIC}| < 7$ means mild evidence against the model with the larger AIC, and $|\Delta\mathrm{AIC}| > 10$ suggests strong evidence against the model with the larger AIC [64]. For the ΔBIC, a range of $0 < |\Delta\mathrm{BIC}| < 2$ also indicates difficulty in preferring the model, and $2 < |\Delta\mathrm{BIC}| < 6$ and $|\Delta\mathrm{BIC}| > 6$ are regarded positive and strong evidence, respectively, against the model with the larger BIC [65]. We find that $\Delta\mathrm{AIC(BIC)} = -4.8(6)$ for the sudden transition M model, and $\Delta\mathrm{AIC(BIC)} = -2.5(8.2)$ for the linear transition M model. It is apparent that the AIC mildly prefers the sudden M transition model, since its value is more than 4 less than that of the constant M model, while the BIC still favors the standard model.

Growth tension. The absolute magnitude of a star is the star's luminosity when it is at a distance of 10 pc. Thus, the difference between the post-transition SNe Ia absolute magnitude M and the pretransition M_0 can be connected with the absolute luminosity L via $M - M_0 = -\frac{5}{2}\log_{10}\frac{L}{L_0}$. Since the peak luminosity of SNe Ia is determined by the mass of nickel synthesized ($m_{\rm Ni}$) [66], we have a simple relation $L \propto m_{\rm Ni} \propto m_c$ after assuming $m_{\rm Ni}$ is directly proportional to the Chandrasekhar mass m_c [67], which can be estimated according to $m_c \simeq \frac{3}{m_e}(\frac{\hbar c}{G_{\rm eff}})^{3/2}$, where m_e is the mass per electron. Then, for a fixed m_e, one has $L \propto G_{\rm eff}^{-3/2}$. Therefore, a change of M found in Sec. II can be explained as a variation of $G_{\rm eff}$. Using $\Delta\mu_G \equiv \mu_G - 1$, where μ_G is defined as $\mu_G \equiv \frac{G_{\rm eff}}{G_N}$ with G_N being the locally measured Newton's constant, to denote the change of $G_{\rm eff}$ and $\Delta M = M - M_0$, we obtain that

$$\Delta\mu_G = 10^{\frac{4}{15}\Delta M} - 1. \tag{6}$$

Obviously, for the case of a sudden transition of M, $\mu_G = 1$ when $z < z_t$ and $\mu_G = 1 + \Delta\mu_G$ when $z \geq z_t$. Using the best-fitting values of A, we have $\Delta\mu_G - 0.076$ and -0.091, respectively, for the sudden and linear transition *Ansätze* of M when $z \geq z_t$. Apparently, both values of $\Delta\mu_G$ are larger than -0.12, which is derived from $\Delta M = -0.2$ assumed in [60].

A variation of μ_G has an impact on the growth rate of the cosmological matter fluctuations $\delta(a) = \frac{\delta\rho}{\rho}(a)$ since the linear growth satisfies the equation

$$\delta'' + \left(\frac{3}{a} + \frac{H'(a)}{H(a)}\right)\delta' - \frac{3}{2}\frac{\Omega_{\rm m0}\mu_G}{a^5 H(a)^2/H_0^2}\delta = 0, \tag{7}$$

where $a = (1+z)^{-1}$ is the scale factor, a prime denotes a derivative with respect to a, ρ is the matter density, and $\delta\rho$ represents the fluctuation of matter density. If one uses parameter σ_8 to quantify the linear growth of the perturbations, the values of σ_8 and $\Omega_{\rm m0}$ derived from the measurements of the weak lensing and galaxy redshift space distortions disagree at about 2σ–3σ level with those inferred from the Planck CMB data [1,68,69]. Now, we discuss what happens to σ_8 and $\Omega_{\rm m0}$ when a modification of μ_G is introduced. To estimate their values, let us note that a commonly observed measurement is the quantity $f\sigma_8$:

$$f\sigma_8 = \frac{\sigma_8}{\delta(a=1)} a\delta'(a, \Omega_{\rm m0}, \mu_G). \tag{8}$$

To obtain δ and δ', we choose the initial conditions to be $\delta(a_{\rm ini} \ll 1) = a_{\rm ini}$ and $\delta'(a_{\rm ini} \ll 1) = 1$ with $a_{\rm ini} \sim 10^{-3}$ [53] and then numerically solve the linear growth equation [Eq. (7)] by using the function scipy.integrate.odeint in Python. In our analysis, 62 observational $f\sigma_8$ data within a redshift range of $0.02 \leq z \leq 1.944$ are used, which are collected in Ref. [54]. The minimum χ^2 method is also used here, which is expressed as

$$\chi^2_{f\sigma_8} = \left[\boldsymbol{f\hat{\sigma}_8}_{\rm obs} - \frac{f\sigma_{8\rm th}}{q}\right]^{\dagger} C^{-1}_{f\sigma_8}\left[\boldsymbol{f\hat{\sigma}_8}_{\rm obs} - \frac{f\sigma_{8\rm th}}{q}\right]. \tag{9}$$

Here, q is the correction factor, dependent on the referenced model of observational data [54], and $C_{f\sigma_8}$ is the covariance matrix of the $f\sigma_8$ sample. Since M varies in $z < 0.02$ and data are located at $z > 0.02$, we thus fix the value of μ_G to be $1 + \Delta\mu_G$ when the two *Ansätze* of varying M are considered.

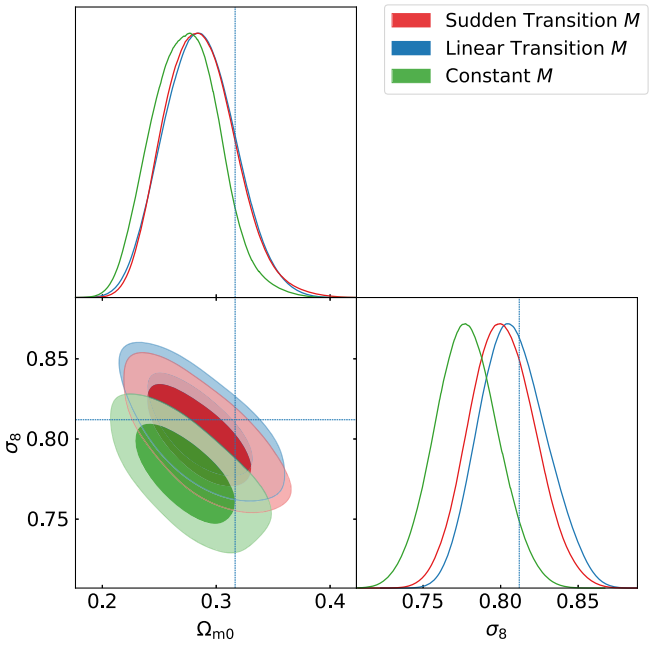

FIG. 2. Constraints on Ω_{m0} and σ_8 from the $f\sigma_8$ data. The blue dotted lines indicate the results from the Planck CMB data.

We find that, when $\mu_G = 1$, the mean values with 1σ uncertainty of the parameters are $\Omega_{m0} = 0.284^{+0.029}_{-0.032}$ and $\sigma_8 = 0.774 \pm 0.020$ with $\chi^2_{\rm min} = 29.016$. The corresponding contour plots on the $\sigma_8 - \Omega_{m0}$ plane are shown in Fig. 2 and Table II. These values deviate significantly from those given by the CMB data at more than 2σ CL, and the marginalized constraint on σ_8 also deviates from the CMB result. When a modified μ_G is considered, we obtain $\Omega_{m0} = 0.286^{+0.028}_{-0.033}$ and $\sigma_8 = 0.801 \pm 0.021$ with $\chi^2_{\rm min} = 28.976$ for the sudden transition *Ansatz* and $\Omega_{m0} = 0.285 \pm 0.031$ and $\sigma_8 = 0.808^{+0.020}_{-0.023}$ with $\chi^2_{\rm min} = 28.970$ for the linear transition one. The contour plots of the constraints on Ω_{m0} and σ_8 with both *Ansätze*, presented in Fig. 2, are close to the CMB result within about 1σ CL, and the marginalized constraints on σ_8 are well consistent with that from the CMB data. Thus, a modified $G_{\rm eff}$ does help resolve the growth tension. Setting the model with $\mu_G = 1$ as the reference one, we also calculate the values ΔAIC(BIC) for both *Ansätze* and find that $\Delta{\rm AIC} = \Delta{\rm BIC} \simeq -0.04$, since all three models have the same free parameters. Therefore, a model favored by the $f\sigma_8$ observational data cannot be singled out by using the AIC and BIC.

Conclusions. We propose a cosmological-model-independent method to obtain the apparent magnitude m and its derivative m' at different redshift points from the SNe Ia data and find that the Pantheon+ sample supports deviation of m and m' from the predictions of the ΛCDM model at the lowest-redshift point. This deviation may be explained as a result of a transition of the absolute magnitude M in the low-redshift region. The observations seem to support this transition, since the minimum value of χ^2 for two *Ansätze* of a varying M is less than that for a constant M. Furthermore, the AIC prefers the model with a sudden transition of M, although the BIC still supports the constant M model. With a varying M, the H_0 tension is alleviated to be about 1σ–2σ, and the growth tension can be resolved after attributing the variation of M to a modification of the effective Newton's constant.

The variation of M or $G_{\rm eff}$ may indicate that the theory of general relativity needs to be extended [70–81]. If the strength of gravity or M evolves over time at very low redshifts, the SNe Ia are no longer standardizable candles, and, thus, the cosmology implied by the existing SNe Ia data will be different [70]. Moreover, a varying $G_{\rm eff}$ not only induces the change in M, but also affects the low-redshift galaxy survey data [82] and the period-luminosity relation in the Cepheid [71,83], as well as the expected fluxes of neutrinos and x rays from neutron stars [84].

Acknowledgments. This work was supported in part by the National Science Foundation of China (NSFC) under Grants No. 12275080 and No. 12075084 and the innovative research group of Hunan Province under Grant No. 2024JJ1006.

[1] L. Perivolaropoulos and F. Skara, New Astron. Rev. **95**, 101659 (2022).
[2] A. G. Riess, Nat. Rev. Phys. **2**, 10 (2020).
[3] R. B. Tully, arXiv:2305.11950.
[4] A. G. Riess *et al.*, Astrophys. J. Lett. **934**, L7 (2022).
[5] Planck Collaboration, Astron. Astrophys. **641**, A6 (2020).
[6] C. D. Huang, A. G. Riess, W. Yuan, L. M. Macri, N. L. Zakamska, S. Casertano, P. A. Whitelock, S. L. Hoffmann, A. V. Filippenko, and D. Scolnic, Astrophys. J. **889**, 5 (2020).
[7] W. L. Freedman, Astrophys. J. **919**, 16 (2021).
[8] N. Khetan, L. Izzo, M. Branchesi *et al.*, Astron. Astrophys. **647**, A72 (2021).
[9] E. Macaulay *et al.*, Mon. Not. R. Astron. Soc. **486**, 2184 (2019).
[10] T. M. C. Abbott *et al.*, Mon. Not. R. Astron. Soc. **480**, 3879 (2018).
[11] D. Camarena and V. Marra, Mon. Not. R. Astron. Soc. **495**, 2630 (2020).
[12] W. Cardona, M. Kunz, and V. Pettorino, J. Cosmol. Astropart. Phys. 03 (2017) 056.

[13] G. Efstathiou, Mon. Not. R. Astron. Soc. **400**, 1138 (2014).
[14] S. M. Feeney, D. J. Mortlock, and N. Dalmasso, Mon. Not. R. Astron. Soc. **476**, 3861 (2018).
[15] B. Follin and L. Knox, Mon. Not. R. Astron. Soc. **477**, 4534 (2018).
[16] A. G. Riess *et al.*, Astrophys. J. **826**, 56 (2016).
[17] A. G. Riess *et al.*, Astrophys. J. **855**, 136 (2018).
[18] A. G. Riess *et al.*, Astrophys. J. **861**, 126 (2018).
[19] B. R. Zhang, M. J. Childress, T. M. Davis, N. V. Karpenka, C. Lidman, B. P. Schmidt, and M. Smith, Mon. Not. R. Astron. Soc. **471**, 2254 (2017).
[20] B. L'Huillier, A. Shafieloo, E. V. Linder, and A. G. Kim, Mon. Not. R. Astron. Soc. **485**, 2783 (2019).
[21] J. Wagner and S. Meyer, Mon. Not. R. Astron. Soc. **490**, 1913 (2019).
[22] B. Wang, M. López-Corredoira, and J.-J. Wei, Mon. Not. R. Astron. Soc. **527**, 7692 (2024).
[23] W. D. Kenworthy, D. Scolnic, and A. Riess, Astrophys. J. **875**, 145 (2019).
[24] V. V. Lukovic, B. S. Haridasu, and N. Vittorio, Mon. Not. R. Astron. Soc. **491**, 2075 (2020).
[25] R. G. Cai, J. F. Ding, Z. K. Guo, S. J. Wang, and W. W. Yu, Phys. Rev. D **103**, 123539 (2021).
[26] J. P. Hu, Y. Y. Wang, J. Hu, and F. Y. Wang, Astron. Astrophys. **681**, A88 (2024).
[27] L. Verde, T. Treu, and A. G. Riess, Nat. Astron. **3**, 891 (2019).
[28] R. Y. Guo, J. F. Zhang, and X. Zhang, J. Cosmol. Astropart. Phys. 02 (2019) 054.
[29] F. Okamatsu, T. Sekiguchi, and T. Takahashi, Phys. Rev. D **104**, 023523 (2021).
[30] G. Alestas, D. Camarena, E. Di Valentino, L. Kazantzidis, V. Marra, S. Nesseris, and L. Perivolaropoulos, Phys. Rev. D **105**, 063538 (2022).
[31] J-P. Hu and F-Y. Wang, Universe **9**, 94 (2023).
[32] K. Jedamzik and L. Pogosian, Phys. Rev. Lett. **125**, 181302 (2020).
[33] L. Hart and J. Chluba, Mon. Not. R. Astron. Soc. **493**, 3255 (2020).
[34] T. Sekiguchi and T. Takahashi, Phys. Rev. D **103**, 083507 (2021).
[35] V. Poulin, T. L. Smith, T. Karwal, and M. Kamionkowski, Phys. Rev. Lett. **122**, 221301 (2019).
[36] K. Jedamzik, L. Pogosian, and G.-B. Zhao, Commun. Phys. **4**, 123 (2021).
[37] J. C. Hill, E. McDonough, M. W. Toomey, and S. Alexander, Phys. Rev. D **102**, 043507 (2020).
[38] E. Rozo *et al.* (DSDD Collaboration), Astrophys. J. **708**, 645 (2010).
[39] D. Rapetti, S. W. Allen, A. Mantz, and H. Ebeling, Mon. Not. R. Astron. Soc. **400**, 699 (2009).
[40] S. Bocquet *et al.* (SPT Collaboration), Astrophys. J. **799**, 214 (2015).
[41] E. J. Ruiz and D. Huterer, Phys. Rev. D **91**, 063009 (2015).
[42] F. Schmidt, Phys. Rev. D **78**, 043002 (2008).
[43] H. Hildebrandt *et al.*, Mon. Not. R. Astron. Soc. **465**, 1454 (2017).
[44] C. Heymans *et al.*, Mon. Not. R. Astron. Soc. **427**, 146 (2012).
[45] S. Joudaki *et al.*, Mon. Not. R. Astron. Soc. **474**, 4894 (2018).
[46] M. A. Troxel *et al.* (DES Collaboration), Phys. Rev. D **98**, 043528 (2018).
[47] F. Köhlinger *et al.*, Mon. Not. R. Astron. Soc. **471**, 4412 (2017).
[48] T. M. C. Abbott *et al.* (DES Collaboration), Phys. Rev. D **98**, 043526 (2018).
[49] T. M. C. Abbott *et al.* (DES Collaboration), Phys. Rev. D **99**, 123505 (2019).
[50] L. Samushia *et al.*, Mon. Not. R. Astron. Soc. **429**, 1514 (2013).
[51] E. Macaulay, I. K. Wehus, and H. K. Eriksen, Phys. Rev. Lett. **111**, 161301 (2013).
[52] A. Johnson, C. Blake, J. Dossett, J. Koda, D. Parkinson, and S. Joudaki, Mon. Not. R. Astron. Soc. **458**, 2725 (2016).
[53] S. Nesseris, G. Pantazis, and L. Perivolaropoulos, Phys. Rev. D **96**, 023542 (2017).
[54] L. Kazantzidis and L. Perivolaropoulos, Phys. Rev. D **97**, 103503 (2018).
[55] D. Scolnic *et al.*, Astrophys. J. **938**, 113 (2022).
[56] D. Brout *et al.*, Astrophys. J. **938**, 110 (2022).
[57] See Supplemental Material at http://link.aps.org/supplemental/10.1103/PhysRevD.110.L021304 for details on our simulation process and results, which test the reliability of our method.
[58] W. D. Kenworthy, A. G. Riess, D. Scolnic, W. Yuan, J. Luis Bernal, D. Brout, S. Casertano, D. O. Jones, Lucas Macri, and Erik R. Peterson, Astrophys. J. **935**, 83 (2022).
[59] L. Perivolaropoulos and F. Skara, Mon. Not. R. Astron. Soc. **520**, 5110 (2023).
[60] V. Marra and L. Perivolaropoulos, Phys. Rev. D **104**, L021303 (2021).
[61] H. Akaike, IEEE Trans. Autom. Control **19**, 716 (1974).
[62] H. Akaike, J. Econom. **16**, 3 (1981).
[63] G. Schwarz, Ann. Stat. **6**, 461 (1978), https://www.jstor.org/stable/2958889.
[64] K. P. Burnham and D. R. Anderson, Sociol. Methods Res. **33**, 261 (2004).
[65] H. Jeffreys, The theory of probability, in *Resonance*, 3rd ed. (Oxford, New York, 1998), https://link.springer.com/article/10.1007/BF02834617.
[66] W. D. Arnett, Astrophys. J. **253**, 785 (1982).
[67] E. Gaztañaga, E. García-Berro, J. Isern, E. Bravo, and I. Domínguez, Phys. Rev. D **65**, 023506 (2001).
[68] E. Di Valentino *et al.*, Astropart. Phys. **131**, 102604 (2021).
[69] E. Abdalla *et al.*, J. High Energy Astrophys. **34**, 49 (2022).
[70] B. S. Wright and B. Li, Phys. Rev. D **97**, 083505 (2018).
[71] Ruchika, H. Rathore, S. R. Choudhury, and V. Rentala, arXiv:2306.05450.
[72] Y-W. Lee, C. Chung, Y. Kang, and M. J. Jee, Astrophys. J. **903**, 22 (2020).
[73] D. Sapone, S. Nesseris, and C. A. P. Bengaly, Phys. Dark Universe **32**, 100814 (2021).
[74] L. Perivolaropoulos and F. Skara, Phys. Rev. D **106**, 043528 (2022).
[75] F. S. Escórcio, J. C. Fabris, J. D. Toniato, and H. Velten, Eur. Phys. J. Plus **138**, 1084 (2023).
[76] D. Camarena and Valerio Marra, arXiv:2307.02434.
[77] P. Mukherjee, K. F. Dialektopoulos, J. L. Said, and J. Mifsud, arXiv:2402.10502.

[78] A. Gómez-Valent, A. Favale, M. Migliaccio, and A. A. Sen, Phys. Rev. D **109**, 023525 (2024).
[79] T. Schiavone, G. Montani, and F. Bombacigno, Mon. Not. R. Astron. Soc. **522**, L72 (2023).
[80] C. Silva, Nucl. Phys. **B998**, 116402 (2024).
[81] S. Vagnozzi, Universe **9**, 393 (2023).
[82] G. Alestas, L. Perivolaropoulos, and K. Tanidis, Phys. Rev. D **106**, 023526 (2022).
[83] J. Sakstein, H. Desmond, and B. Jain, Phys. Rev. D **100**, 104035 (2019).
[84] I. Goldman, arXiv:2402.09859.